Infrared Physics & Technology 54 (2011) 204–208

Contents lists available at ScienceDirect

Infrared Physics & Technology

journal homepage: www.elsevier.com/locate/infrared

Modelling of electronic transport in Quantum Well Infrared Photodetectors

Virginie Trinité [a,*], Ezzeddine Ouerghemmi [a], Vincent Guériaux [b], Mathieu Carras [b], Alexandru Nedelcu [b], Eric Costard [b], Julien Nagle [a]

[a] THALES Research & Technology, Campus Polytechnique, 1, Avenue Augustin Fresnel, RD 128, 91767 Palaiseau cedex, France
[b] Alcatel Thales III–V Lab, Campus Polytechnique, 1, Avenue Augustin Fresnel, 91767 Palaiseau, France

ARTICLE INFO

Article history:
Available online 13 January 2011

Keywords:
Quantum Well Infrared Photodetectors
models
III–V Semiconductors
Gallium arsenide
Dark conductivity

ABSTRACT

Our interest is to model the electronic transport in Quantum Well Infrared Photodetectors (QWIPs). Standard modelling was based on self-consistent calculation of the non-uniform electric field with empirical description of the electron capture (Thibaudeau et al., 1996 [17]). Realistic empirical parameters had to be extracted from experiment, consequently purely numerical studies were not possible. Moreover, this approach allowed only a qualitative description of transport phenomena. In order to get rid of adjustable parameters, we have changed for a modelling based on the microscopic description of the transport (Jovanović et al., 2004 [11]). We have applied this modelling to the design of a variety of QWIPs. For example, excellent agreement with experimental dark current–voltage curves for different sizes of the barriers is demonstrated on a 8 μm detector over more than 6 orders of magnitude. The behaviour with respect to temperature on a wide range (30–200 K) is also well reproduced on this device as well as on a 17 μm detector. Those promising results confirm that this approach can give not only a good quantitative agreement but can also be a useful predictive tool.

1. Introduction

In this article we will present the modelling of the electronic transport in multiquantum well structures based on semiclassical Boltzmann-like equations [10]. In our previous modelling, the main empirical parameter was the capture probability [17]. However the values were difficult to extract from experiment and the dependency with the structure parameters remained nearly unknown. This problem, combined with other approximations, gave only a qualitative understanding of the physics of the electronic transport in the thermal regime, but no predictive results. A new type of modelling, based on a fully quantum-mechanical model, was first proposed by Harrison et al. [2,4,11,12]. This type of modelling, without parameters based on microscopic quantum description of the scattering from state to state, are very appealing and have proven their efficiency to describe other types of quantum structures like the quantum cascade laser (QCL) [8,16]. The specificity of the QWIP is that the electronic transport is mediated by extended states in the conduction band as opposed to QCLs in which it is mediated by localized states. Up to now, very few work has been devoted to the validation of this approach for QWIPs.

Thanks to the long experience of III–V Lab in the QWIPs field, we have been able to compare numerical results and experimental data for a large number of quantum designs. Our conclusion is that this approach can describe quantitatively the current in QWIPs within a large range of external parameters (temperature and bias) excepted at very low temperatures and voltage. The first part of this work is dedicated to the presentation of the modelling, the second one to the convergence study and the last one to the comparison with experiment in dark condition (no incoming photons).

2. Theory

The general form of the structures we want to study consists in a large number of periods (typically >20) containing different material layers. For sake of simplicity, the modelling we present here is periodic. We have thus to keep in mind that there will be no finite size effects. In particular the effect of the injection contact is not accounted for. This approximation suits well to structures like QCLs or QCDs, where the field is homogeneous. However, in the case of QWIPs, it is well known that it is not the case [17]. In fact, the inhomogeneity is not so important in dark conditions when the number of periods is large enough. In our test structure, the period is simply a well of GaAs and a barrier of $Al_xGa_{1-x}As$. The implementation of the model has four main steps that we will explain in the following: (i) Wavefunctions calculation, (ii) Wavefunctions selection, (iii) Scattering rates, (iv) Rate equation solving and current calculation. Since step three requires the knowledge of the population which is

* Corresponding author.
E-mail address: virginie.trinite@thalesgroup.com (V. Trinité).

1350-4495/$ - see front matter © 2011 Elsevier B.V. All rights reserved.
doi:10.1016/j.infrared.2010.12.014

a result of step four, we perform a self-consistent calculation on those two steps.

(i) Wavefunction calculation: The hamiltonian of the conduction band is solved in the envelope function approximation and we take into account its non parabolicity as reported in Ref. [15].

$$p_z \frac{1}{2m^*(e_i,z)} p_z \phi_i(z) + V_{BC}(z)\phi_i(z) = e_i \phi_i(z) \quad (1)$$

$$\frac{1}{m^*(e,z)} = \frac{1}{3m_0}\left(\frac{2E_p}{e_c(z)+E_g} + \frac{E_p}{e_c(z)+E_g+\Delta_{so}}\right) \quad (2)$$

$$e_c(z) = e - V_{BC}(z) \quad (3)$$

with E_p the Kane energy as in Ref. [15], m_0 the electro mass, E_g the gap and Δ_{so} the split-off energy. $\phi_i(z)$ is the envelope function along the growth axis for $k_{//} = 0$.

The resolution of this equation above the barriers would require a continuum of electron states. For a finite calculation, we need to discretize the continuum. This is straightforwardly done by using hard wall boundary conditions (see Fig. 1) which consist in solving the Eq. (2) for a finite number of periods N surrounded by two barriers conveniently chosen. When N increases the calculation becomes more precise and time consuming.

Due to the periodicity of the structure, the wavefunctions obey a spatial and energy translation symmetry: if $\phi_i(z)$ is a solution with energy e_i then for any p relative integer $\phi_i(z + pD)$ should be a solution at the energy $e_i + p\Delta V$, with D the length of one period and ΔV the potential drop across one period. Thus a finite number of wavefunctions can describe the whole structure by applying this translation symmetry, which greatly simplifies the problem. This symmetry is broken in the method for solving the Schrödinger equation by the use of hard boundaries. This implies that if we want to ensure periodic boundary condition, we have to impose the symmetry. The states of the central period are the closer to the ideal periodic case. We will take them as our finite set of wavefunctions mentioned above (see Fig. 1).

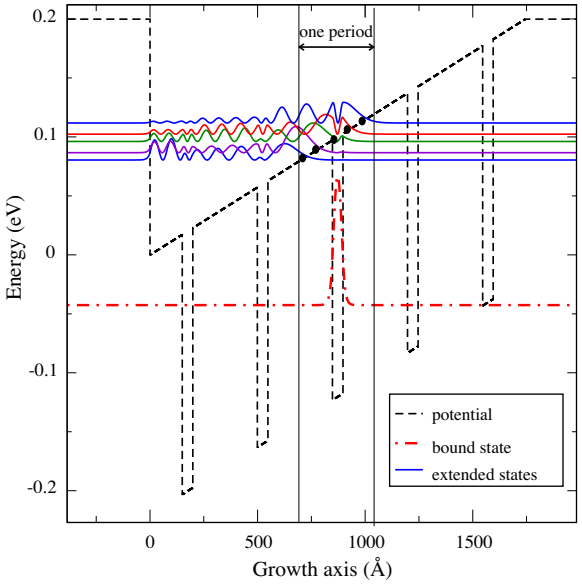

Fig. 1. Example of potential used for solving the Schrödinger equation (sample LWD, 5 periods, voltage/period = 0.04 V) and the wavefunctions associated (we have plotted $5|\phi_i(z)|^2 + e_i$ for the sake of clarity). The vertical lines show the central period. The dark points show how the extended states are sorted by period.

(ii) Wavefunctions selection: In order to select the states of the central period, we have to assign each eigenstate solution of the hard wall boundary condition to its dedicated period. For bound eigenstates, it is easy to do, by calculating the mean position z^i_{mean} of the wavefunction i: the wavefunction is selected if z^i_{mean} is in the central period. A wavefunction belongs to a bound state if the standard deviation of its position is smaller than a well chosen value. For the other states, named continuum states, it is not so straightforward, as they are not confined at a defined position. Jovanovic et al. [12] use the overlap of the continuum wavefunction with the period to select the states. We prefer another criterion, which is more robust for homogeneous field: we calculate the crossing point, solution of $e_i = V_{BC}(z_{cross})$ as illustrated in Fig. 1. If z_{cross} is in the central period we consider that the continuum wavefunction belongs to this period.

(iii) Scattering rates: Knowing the available electronic states we can now address the dynamics of carriers. In this model the transport is dominated by incoherent scattering, so we can use semiclassical Boltzmann-like equation [10]: transport is controlled by scattering occurring between eigenstates. For each eigenstate we can write a rate equation as

$$\frac{dn_i}{dt} = \sum_j \Gamma_{ji}(n_j, n_i) - \Gamma_{ij}(n_i, n_j) \quad (4)$$

with $\Gamma_{ij}(n_j, n_i)$ the total scattering rate from state i to state j. j and i run over all states of the structure. The total scattering rate is defined as:

$$\Gamma_{ji}(n_j, n_i) = \sum_{mechanism} \Gamma^{scatt}_{i,j}(n_i, n_j) \quad (5)$$

The scattering rate $\Gamma^{scatt}_{i,j}(n_i, n_j)$ is calculated with the Fermi's golden rule, and we assume thermalised carrier distribution in each subband [7,9]. As a result only the populations of the subbands enter the balance rate equations. Indeed individual k-space scattering mechanism are averaged on each subband thanks to the use of the Fermi–Dirac statistics $f(E, T_e) = \frac{1}{1+e^{\frac{E}{kT_e}}}$ at an electronic temperature T_e. Because of the use of the Fermi–Dirac statistics, the rate $\Gamma^{scatt}_{i,j}$ depends on the population of the initial and final subbands n_i and n_j trough their Fermi-level, μ_i and μ_j:

$$\Gamma^{scatt}_{i,j}(n_i, n_j) = \frac{2\pi}{\hbar} \sum_{k'k} |\langle \phi_i | H^{scatt} | \phi_j \rangle|^2 \delta\left(e^{k'}_i - e^k_j\right) f\left(e^{k'}_i, T_e\right)\left(1 - f\left(e^k_j, T_e\right)\right) \quad (6)$$

with $e^k_j = e_j + \frac{\hbar^2 k^2}{2m^*_i} = e_j + \epsilon_k$. and

$$\rho^i_{2D} \int_0^\infty f(\epsilon_i + \epsilon_k - \mu_i, T_e) d\epsilon_k = n_i \quad (7)$$

$\rho^i_{2D} = \frac{m^*_i}{\pi\hbar^2}$ is the 2 D density of state i. Wavefunctions are calculated by taking into account the non parabolicity, so that m^*_i are not constant (see Eq. (3)), but we discard this dependency for the calculation of the rate $\Gamma^{scatt}_{i,j}$ and the calculation of the Fermi-level and use a constant m^*_i taken to be the average value of $m^*(e, z)$:

$$m^*_i = \int_{-\infty}^{+\infty} \phi_i(z)^* m^*(e_i, z) \phi_i(z) dz \quad (8)$$

With this approach we can describe the scattering of the electrons by LO-phonon emission and absorption, LA-phonon emission and absorption, alloy disorder, ionized impurities, interface roughness and photon emission and absorption. However in this article ionized impurities are not calculated since it is time consuming and